Effective Velocity of Transport in Curved Wall Boundary Layers

S. K. Hong* and S. N. B. Murthy†
Purdue University, West Lafayette, Indiana

An alternative to simple gradient diffusion hypothesis for turbulence transport in a boundary layer is the finite velocity of transport hypothesis. The applicability and implications of the latter are examined utilizing a simple and direct framework, the large eddy interaction model with eddy-eddy interactions accounting for anisotropic transport, in the case of five variously curved wall boundary-layer flows. The development of the turbulence structure including orientation of large eddies is predicted along the flow. It is also shown that the Large Eddy Interaction Model framework explains the manner in which turbulence relaxes following sudden curvature removal.

Introduction

THE development of turbulence models for computational fluid dynamics continues to be a subject of great interest. A number of entry points into the literature on turbulence modeling can be found in Refs. 1-4. The commonality and levels of sophistication in models can be realized by dividing them into 1) large eddy simulation models and 2) others based on modeling specific processes, or terms in the basic equations, governing mean and fluctuating quantities: eddy-viscosity,[5] two equations for the turbulent kinetic energy and rate of dissipation (k-ϵ),[6] or for the energy and vorticity densities (e-ω),[7] and algebraic stress[8] models, for example. One important consideration is then the manner in which one can establish the validity and applicability of the individual models. Since this cannot be accomplished by an appeal to the models themselves, the development of an independent framework by means of which specific aspects of turbulence processes can be assessed and tested in given flows, in a simple and direct fashion, becomes of some value.

Two major turbulence processes that require modeling in all classes of flows are 1) turbulent diffusion and 2) pressure fluctuation-related processes. A framework called the Large Eddy Interaction Model (LEIM) has been developed to examine the preceding two processes.[9] The basis of the framework and its applicability for assessing turbulent diffusion in the case of the boundary-layer flow past curved walls have been described in part in Ref. 10. The boundary-layer flow past a curved wall provides a simple example of an inhomogeneous shear layer subjected to a complex strain; anisotropy in transport and redistribution of stresses through the action of pressure fluctuations become important features in such flows. It is the objective in the following to examine nongradient-type modeling for turbulent transport in contrast to gradient diffusion utilized earlier.[10] The application of the LEIM for the study of currently adopted procedures for modeling pressure-strain correlations has been discussed in Ref. 11.

Presented as Paper 84-0177 at the AIAA 22nd Aerospace Sciences Meeting, Reno, NV, Jan. 9-12, 1984; received Jan. 4, 1985; revision received June 12, 1985.

*Research Assistant, School of Aeronautics and Astronautics; currently, NRC Research Associate, NASA Ames Research Center, Moffett Field, CA. Member AIAA.

†Senior Researcher, School of Mechanical Engineering. Member AIAA.

Gradient and Nongradient Transport Models

Simple gradient diffusion models have been reasonably successful in predicting homogeneous flows and boundary-layer flows wherein departure from "equilibrium" state is not severe. Various proposals for improving gradient-type models for transport have been made by including higher-order terms as a correction to the first-order term. Such modifications, however, still do not account for the various governing physical processes and considerations.[12]

As an alternative, Bradshaw et al.[13] and Townsend[14,15] have suggested utilization of a "velocity scale" to relate turbulent diffusion to the intensity of local velocity fluctuations. The transport of turbulent stresses is then viewed in terms of a convection process with a "finite velocity scale" characteristic of the given flowfield. Such a model may be considered as belonging to the general class of diffusion models[16] represented by the following expression:

$$F(x_i,t)=fn\left(\Gamma,\ \frac{\partial\Gamma}{\partial t},\ \frac{\partial\Gamma}{\partial x_i},\ \frac{\partial^2\Gamma}{\partial x_i^2},\ldots\right) \tag{1}$$

where Γ represents "intensity" of a turbulence field and F is a functional of Γ. Equation (1) should be interpreted to imply that the simple gradient diffusion model, the higher-order gradient diffusion models, and the finite velocity transport model may be applicable in different parts of a particular shear layer or to different shear layers under various governing conditions of flow. In the following, the applicability and implications of the use of a finite velocity transport model to the outer part of curved wall boundary layers are discussed.

Framework

The LEIM is based on the following: 1) decomposing the velocity fluctuations into orthonormal functions, 2) constructing dynamical equations for those functions, 3) identifying the first eigenmode—i.e., the solution of the dynamical equation—as a large eddy,[17] and 4) examining the development of the large eddy in the context of its interaction with the mean flow and the eddy-eddy interactions by utilizing a dynamical equation for velocity fluctuation. The dynamical equation includes the effect of pressure fluctuation, which can be represented by the Poisson equation.

Large Eddy Interaction Model

The velocity fluctuation u_i may be represented as the sum of a Fourier series involving orthonormal functions, $\phi_i^{(n)}$,

i.e.,

$$u_i(\bar{x},t) = \sum_{n=1}^{\infty} \alpha_n \phi_i^{\{n\}}(\bar{x},t) \tag{2}$$

where α_n is a random coefficient and n an integer. Based on momentum balance, one can obtain a dynamical equation for the nth eigenmode as first given by Lumley.[17] For the first mode, which is found to be dominant over all other modes,[18,19] the dynamical equation, under incompressible flow assumptions, becomes the following in a time-averaged sense:

$$U_j \frac{\partial \phi_i^{(1)}}{\partial x_j} + \frac{\partial U_i}{\partial x_j}\phi_j^{(1)} + \frac{\partial}{\partial x_j}\left\{ \sum_{p,}^{\infty} \sum_{q=1}^{\infty} \frac{\overline{\alpha_1^* \alpha_p \alpha_q}}{\lambda^{(1)}} \phi_i^{\{p\}} \phi_j^{\{q\}} \right\} = \frac{\partial \pi^{(1)}}{\partial x_i} + \nu \frac{\partial^2 \phi_i^{(1)}}{\partial x_j^2} \tag{3}$$

where $\lambda^{(1)} \equiv \overline{\alpha_1^* \alpha_1}$; the asterisk denotes a complex conjugate and U_i is the mean velocity. The indexes $i = 1,2,3$ represent the streamwise direction x, the local normal to the wall y, and the spanwise direction z, respectively, in the case of a boundary-layer flow. For the pressure fluctuation, $\pi^{(1)}$, one can obtain the Poisson equation imposing the continuity relation; thus,

$$\frac{\partial^2 \pi^{(1)}}{\partial x_j^2} = 2\frac{\partial U_j}{\partial x_k}\frac{\partial \phi_k^{(1)}}{\partial x_j} + \frac{\partial^2}{\partial x_k \partial x_j}\left\{ \sum_{p,}^{\infty} \sum_{q=1}^{\infty} \frac{\overline{\alpha_1^* \alpha_p \alpha_q}}{\lambda^{(1)}} \phi_j^{\{q\}} \phi_k^{\{p\}} \right\} \tag{4}$$

The nonlinear term appearing in Eqs. (3) and (4) represents the interaction process between eddies of various sizes and requires modeling in view of involvement of higher-order modes, $\phi_i^{(2)}, \phi_i^{(3)}, \ldots$. This is the only modeling required in the LEIM.

The LEIM bears some resemblance to the so-called rapid distortion theory and its recent developments.[15,20,21] It may be pointed out that the LEIM presents a means of analyzing inhomogeneous flows, basically in a time-averaged sense. It is a diagnostic tool and not a means of predicting the turbulent flowfield. The mean flow is assumed to be known and the modeling of eddy-eddy interactions becomes specialized for each flow. On the other hand, in principle one can solve the momentum equation for mean flow simultaneously with that for the fluctuating component and obtain the mean flow. It would then become necessary to solve the dynamical equations for $\sqrt{\lambda^{(n)}}\phi_i^{\{n\}}$ $(n = 1,2,3,\ldots)$,[22] noting that the Reynolds stress becomes

$$\overline{u_i u_j}(\bar{x},t) = \sum_{n=1}^{\infty} \lambda^{(n)} \phi_i^{\{n\}} \phi_j^{\{n\}}(\bar{x},t) \tag{5}$$

Some judgment becomes necessary on the number of modes (n) to be included. In the current paper, the objective is to test the applicability of a particular model for eddy-eddy interactions to selected flow cases. Attention has been focused on the first mode and changes in its structure in relation to turbulence quantities of engineering interest.

Assuming that a form of "bulk convection" may play a major part in turbulent transport, leading to a "finite velocity scale" of transport (FVT) hypothesis, the nonlinear eddy-eddy interaction terms can be reduced to leading order as follows:

$$-\sum_{p,}^{\infty} \sum_{q=1}^{\infty} \frac{\overline{\alpha_1^* \alpha_p \alpha_q}}{\lambda^{(1)}} \phi_i^{\{p\}} \phi_j^{\{q\}} = v_{ij}\phi_j^{(1)} + v_{ji}\phi_i^{(1)} \tag{6}$$

where the anisotropic velocity scale v_{ij} represents the transport of energy density from a large eddy to eddies of smaller sizes through their interactions. On the other hand, if one follows the analogy of Boussinesq,[23] the simple gradient diffusion (SGD) hypothesis yields

$$-\sum_{p,}^{\infty} \sum_{q=1}^{\infty} \frac{\overline{\alpha_1^* \alpha_p \alpha_q}}{\lambda^{(1)}} \phi_i^{\{p\}} \phi_j^{\{q\}} = \epsilon_{ik}\frac{\partial \phi_k^{(1)}}{\partial x_j} + \epsilon_{jk}\frac{\partial \phi_k^{(1)}}{\partial x_i} \tag{7}$$

where ϵ_{ij} is the anisotropic eddy viscosity. In contrast to the FVT hypothesis, the SGD hypothesis implies a velocity scale of infinite magnitude.[24]

It can be shown that the dynamical equation becomes hyperbolic in nature when the FVT hypothesis is employed, provided additional assumptions are introduced as follows: 1) the effect of the viscous term is small and 2) the mean flow field is known from experiment or other source. Thus, upon substituting Eq. (6) into Eq. (3), one obtains a linear, hyperbolic equation for $\phi_i^{(1)}$; namely,

$$U_j \frac{\partial \phi_i^{(1)}}{\partial x_j} + \frac{\partial U_i}{\partial x_j}\phi_j^{(1)} - \frac{\partial}{\partial x_j}\{v_{ij}(\phi_i^{(1)} + \phi_j^{(1)})\} = \frac{\partial \pi^{(1)}}{\partial x_i} \tag{8}$$

On the other hand, the use of the SGD hypothesis leads to an elliptic dynamical equation that can be reduced to a parabolic form under the assumption; namely, the characteristic length scale in the main flow direction is much larger than that in the transverse direction.

It is assumed that the turbulent part of the boundary layer may be divided into two parts: 1) the inner part close to the wall where gradient diffusion hypothesis may be expected to apply, and 2) the outer part where the FVT hypothesis may apply. Regarding the latter, it is identified as the region where viscous effects are negligibly small.

LEIM Procedure

In any turbulent shear flow where mean velocities are two-dimensional, $(U,V,0)$, such as in streamwise curved wall boundary layers, a Fourier transform is applicable. Considering a time-averaged structure, the spectral functions may be defined as follows:

$$\hat{\phi}_i(x,y,k_3) = \frac{1}{2\pi}\int_{-\infty}^{\infty} \phi_i^{(1)}(x,y,z)\exp(-\hat{i}k_3 z)\,dz \tag{9}$$

$$\hat{\pi}(x,y,k_3) = \frac{1}{2\pi}\int_{-\infty}^{\infty} \pi^{(1)}(x,y,z)\exp(-\hat{i}k_3 z)\,dz \tag{10}$$

where k_3 is the one-dimensional wave number. Substituting those into Eq. (8) and dividing the resulting complex equations into real and imaginary parts by writing

$$\hat{\phi}_1 = P_1 + \hat{i}P_2, \quad \hat{\phi}_2 = P_3 + \hat{i}P_4$$
$$\hat{\phi}_3 = P_5 + \hat{i}P_6, \quad \hat{\pi} = P_7 + \hat{i}P_8 \tag{11}$$

one obtains two sets of equations; namely, one for (P_1, P_3, P_6, and P_7) and a second for (P_2, P_4, P_5, P_8). Although it may appear necessary to solve both sets of equations, only the group of equations for (P_2,P_4,P_5,P_8) is selected for further analysis based on the following analytical and physical considerations. Analytically, the differences between the two groups of equations arise only in the sign of certain small terms which represent parts of eddy-eddy interactions or transport. Physically, if the large eddies are treated as long cylindrical structures (Ref. 14, p. 247), the large eddy velocity components u and v can be represented by odd functions and the component w by an even function, which is consistent with the choice of the group of equations for P_2, P_4, and P_5. Those equations are hyperbolic in nature.

Regarding P_8, an equation can be obtained by the Fourier transform of Eq. (4). However, if such an equation is replaced by a prescribed pressure fluctuation field, then an important advantage arises in that only the set of hyperbolic equations for P_2, P_4, and P_5 needs to be solved.

The contribution to the three normal stresses from the first mode, $\phi_i^{(1)}$, can then be expressed as follows utilizing Eqs. (5) and (9):

$$\overline{u_i^2}(x,y) = \lambda^{(1)} \int_{-\infty}^{\infty} \Phi_{ii}(x,y,k_3)\,dk_3 \tag{12}$$

with

$$\Phi_{ii}^*(k_3) = \hat{\phi}_i(k_3)\hat{\phi}_i^*(k_3) \tag{13}$$

where Φ_{ii} is the spectrum of the double velocity correlation, $R_{ii} = \overline{u_i(z)u_i(z+r_3)}$. It may be observed that $\lambda^{(1)}$, the energy of the first mode, is still undetermined. However, utilizing P_2, P_4, and P_8, the following structural quantities can also be calculated: 1) turbulent normal stress profiles; 2) normal stress intensities $(\overline{u_i^2}/\overline{q^2})$, where $\overline{q^2} = (\overline{u^2} + \overline{v^2} + \overline{w^2})$; 3) shear-stress intensity $(\overline{uv}/\overline{q^2})$; 4) orientation of the principal axes of the large eddies (ϕ), which is given by $\phi = \frac{1}{2}\tan^{-1}[-2\overline{uv}/(\overline{u^2} - \overline{v^2})]$; and 5) changes of anistropy $(\overline{u^2}/\overline{v^2})$. For the shear-stress correlation, a correlation coefficient C_s is introduced, where $C_s \equiv -\overline{uv}/(\sqrt{\overline{u^2}}\sqrt{\overline{v^2}})$. It may be observed that $C_s = 0.5$ in the case of a flat plate.[25] In the case of curved flows, the value of C_s is determined[10] again based on experimental results.

Application to Curved Flows

The LEIM has been applied to four streamwise curved wall flow cases that have received partial acceptance in the 1980-81 AFOSR-Stanford Conference, and the predicted results have been satisfactory in comparison with experimental data and also provide some insight into the manner in which a turbulence structure changes over a curved wall.[10]

The objective is to predict turbulence quantities in the boundary layer over variously curved walls at various stations (angles of turning). The boundary layer at any location along the wall is divided into three parts: the outer layer, the intermediate layer, and the viscous sublayer.[9] The FVT hypothesis is considered[13] applicable over most of the boundary layer, except in the inner layer where viscosity effects dominate.

In order to solve Eq. (8), one needs 1) local mean velocity distributions and 2) the distribution of velocity scales in the outer part of the boundary layer. Regarding item 1, experimental data are utilized. Regarding item 2, an exponential variation is assumed, namely,

$$v_{i2} = a_i \exp(-b_i \xi^m) \tag{14}$$

where a_i and b_i are functions of geometry, $\xi \equiv y/\delta$, δ is the local boundary-layer thickness, and m an appropriate integer. Given the mean flow distributions, the numerical values of a_i and b_i are determined based on the best agreement of the predicted distributions of $\overline{u^2}$, $\overline{v^2}$, and $\overline{w^2}$ with the distributions obtained from experimental measurements. In practice, the values of a_i and b_i have been determined first for the case of the boundary layer over a flat plate utilizing the measurements given by Klebanoff.[25] Then, based on those results, velocity scales for curved flows have been determined utilizing corresponding mean velocity profiles. The velocity scales applicable in the initial part of a curved wall require some adjustment as the wall is turned further; i.e., the values of a_i and b_i determined for the initial region of turning will need changes before predictions can match experimental data in regions of greater turning.

Test Cases

The following—one flat-plate case and four curved-flow cases—have been chosen for analysis:

1) flat plate—Klebanoff[25]
2) mild convex—Ramaprian and Shivaprasad[26,27]
3) strong convex—Gillis et al.[28]
4) mild concave—Ramaprian and Shivaprasad[26,27]
5) strong concave—So and Mellor[29]

Flow conditions for the five test cases are summarized in Table 1. The Reynolds number based on boundary-layer thickness $U_0\delta/\nu$ is of $\mathcal{O}(10^4)$ in all cases.

Calculation Procedure

The region of applicability of the FVT hypothesis is considered as the outer part of the boundary layer bound by its outer edge and a chosen location within, where boundary conditions need to be prescribed. In the calculation procedure adopted here, an inner boundary-layer region adjacent to the wall is assumed to be governed by a set of equations for P_2, P_4, P_5, and P_8, wherein transport is modeled on the basis of gradient diffusion; the resulting system of parabolic equations has been presented in Table 2 of Ref. 10. An implicit upwind differencing method can be applied for solving that set of equations. The outer boundary-layer region, which is the region of principal interest here, is described by the system of hyperbolic equations for which the method of Courant et al.[30] is employed for numerical analysis. The system of parabolic equations resulting from the SGD hypothesis is solved first in the region $0 \le y/\delta \le 1$, utilizing selected values for transport coefficients C_1, C_2, and C_3 in the eddy-viscosity formula,

$$\epsilon_{ij} = (C_i \ell)^2 \frac{\partial U}{\partial y}\delta_{ij} \tag{15}$$

where ℓ is an integral length scale of turbulence. Solutions for the pressure fluctuation, $P_8(x,y,k_3)$, are retained from the calculation for the entire boundary layer. The value of P_8 is therefore treated as a prescribed quantity everywhere in the outer layer. For given initial and boundary conditions, one can then undertake solution of the hyperbolic equations for P_2, P_4, and P_5 governing the outer layer. The solution has been obtained in all cases in the region $0.2 \le y/\delta \le 1.0$, the choice of the extent of the region into the boundary layer being arbitrary. It has been found by trial-and-error that eight equally spaced values in the logarithmic scale for k_3, in

Table 1 Flow conditions for the test cases

Cases	$C = 1/R$, 1/m	U_0, m/s	θ_1, deg	δ_1, cm	θ_2, deg	δ_2, cm	Re, $\times 10^{-4}$
Flat plate[25]	0.0	15.2	—	7.62	—	—	7.5
Mild convex[26,27]	0.4	22.1	2.0	2.35	22.0	2.96	3.5
Strong convex[28]	2.22	16.0	20.0	3.86	80.0	4.49	4.0
Mild concave[26,27]	−0.39	22.0	2.0	2.47	22.0	3.79	3.6
Strong concave[29]	−2.0	21.6	35.0	3.30	109.0	5.60	4.7

NB: Subscripts 1 and 2 denote the first and the last measurement stations, respectively, along the curved wall. $Re \equiv U_0\delta/\nu$, $\delta = \delta_1$.

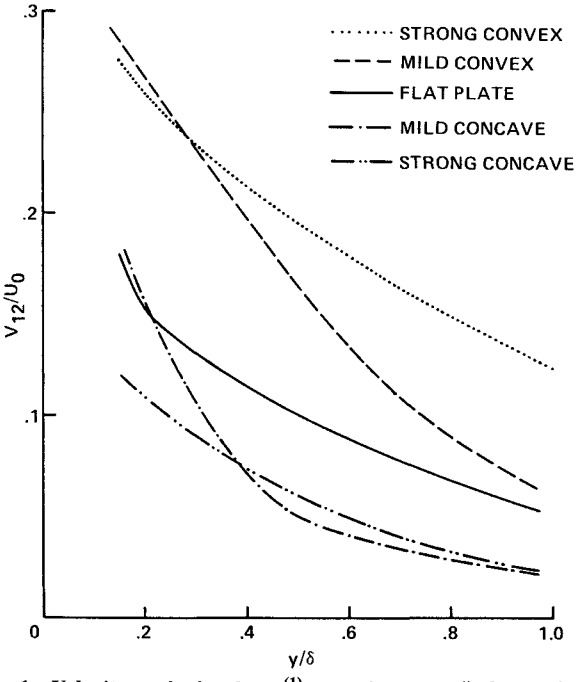

Fig. 1 Velocity scale in the $\phi_1^{(1)}$ equation vs y/δ for variously curved flows.

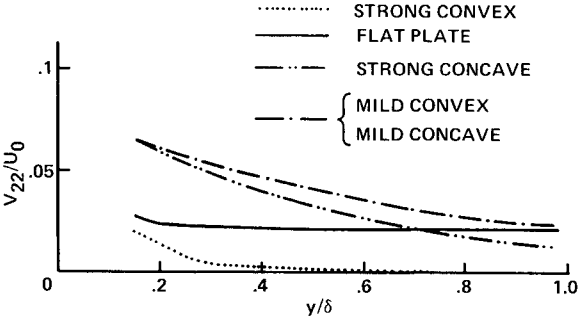

Fig. 2 Velocity scale in the $\phi_2^{(1)}$ equation vs y/δ for variously curved flows.

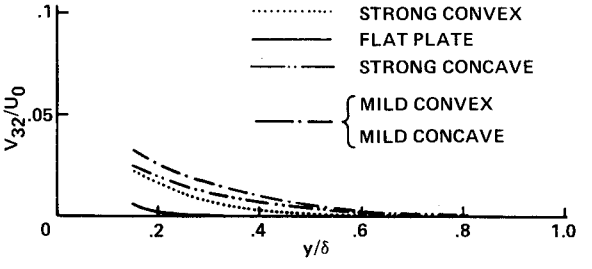

Fig. 3 Velocity scale in the $\phi_3^{(1)}$ equation vs y/δ for variously curved flows.

the range of $0.05 \leq k_3 \leq 10.0$ (1/cm), together are adequate to yield the desired turbulence quantities within acceptable errors in comparison with experimental data in all of the test cases.

Results

Figures 1-3 show the velocity scales that yield the best agreement between predictions and measurements for the five cases currently investigated. The values of v_{12} shown in Fig. 1 and associated with the $\phi_1^{(1)}$ equation are higher for convex flows and lower for concave flows compared with those for the flat-plate case. The distribution of v_{22} shows the opposite from that of v_{12} with respect to curvature. In Fig. 2, values of v_{22} are lower for convex flows and higher for concave flows compared to the flat-plate value. The effect of curvature on v_{32} values, as shown in Fig. 3, is approximately the same in all cases.

Predicted results for normal stress components and three structural quantities for flows over the flat plate and the mild convex, strong convex, mild concave, and strong concave walls are presented as follows:

1) Figure 4 shows the distribution of $\overline{v^2}$ normalized by the local maximum intensity as a function of y/δ in the five test cases. In the figure, θ denotes the angle of turning and s the distance along the curved wall. (Similar distributions have been predicted for $\overline{u^2}$ and $\overline{w^2}$, but are not included here for brevity.) The strong wall curvature suppresses the $\overline{v^2}$ profile of the convex flow and swells that of the concave case, so that the peak of normal stress occurs in the latter case in the middle of the boundary layer.

2) Figures 5-9 provide the shear intensity ($\overline{uv}/\overline{q^2}$), orientation of the principal axes ϕ, and a measure of anisotropy ($\overline{u^2}/\overline{v^2}$). The rotation of the principal axes of stress increases with negative (concave) curvature and decreases with positive curvature. The amount of rotation is suppressed further on the convex wall and is enhanced on the concave wall with increasing y in both cases. The results of the change in anisotropy show that turbulence on a convex wall tends toward greater anisotropicity than that on a concave wall; the anisotropicity of strongly convex flow is nearly twice the value of strongly concave flow.

In general, one can observe the satisfactory nature of predictions obtained with the LEIM, the chosen transport scales, and the stress correlation coefficients in comparison with the experimental data.

Hyperbolic Nature of the Governing Equations

The system of first-order partial differential equations for P_2, P_4, and P_5, which are hyperbolic, can be written in the following form:

$$[A]\begin{bmatrix} \frac{\partial P_2}{\partial y} \\ \frac{\partial P_4}{\partial y} \\ \frac{\partial P_5}{\partial y} \end{bmatrix} + [B]\begin{bmatrix} \frac{\partial P_2}{\partial x} \\ \frac{\partial P_4}{\partial x} \\ \frac{\partial P_5}{\partial x} \end{bmatrix} + \begin{bmatrix} f_1(P_2,P_4,P_5,P_8) \\ f_2(P_2,P_4,P_5,P_8) \\ f_3(P_2,P_4,P_5,P_8) \end{bmatrix} = 0 \tag{16}$$

where

$$[A] = \begin{bmatrix} V-v_{12} & -v_{12} & 0 \\ 0 & V-2v_{22} & 0 \\ 0 & -v_{32} & v_{32} \end{bmatrix} \tag{17}$$

$$[B] = \begin{bmatrix} U/(1+Cy) & 0 & 0 \\ 0 & U/(1+Cy) & 0 \\ 0 & 0 & U/(1+Cy) \end{bmatrix} \tag{18}$$

$C = 1/R$ and R is the radius of wall curvature.

Writing

$$|[A] - \lambda[B]| = 0 \tag{19}$$

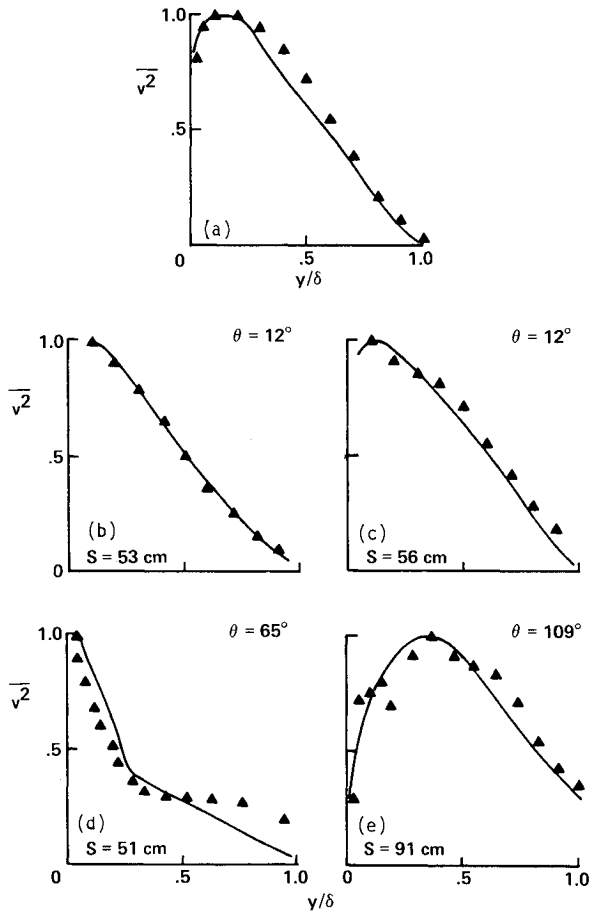

Fig. 4 Normalized $\overline{v^2}$ profiles predicted based on the FVT hypothesis vs y/δ for the cases of a) flat plate, b) mild convex, c) mild concave, d) strong convex, and e) strong concave.

three roots, λ_1, λ_2, and λ_3, are found as follows:

$$\lambda_1 = (1+Cy)(V-v_{12})/U \tag{20}$$

$$\lambda_2 = (1+Cy)(V-2v_{22})/U \tag{21}$$

$$\lambda_3 = (1+Cy)(V-v_{32})/U \tag{22}$$

Thus, λ_1, λ_2, and λ_3 are real values but become identical when $v_{12} = 2v_{22} = v_{32}$. The only condition for the system of equations (16) to be hyperbolic is that

$$v_{12} \neq 2v_{22} \neq v_{32} \tag{23}$$

Existence of Characteristic Field Velocity

The three roots found from the determinantal equation, Eq. (19), can be identified as characteristics of the system of equations, Eq. (16).

Two of the characteristics, λ_1 and λ_2, from a wedge in the x,y plane whose characteristic angle γ_{12} becomes, approximately, the following:

$$\gamma_{12} = \frac{(1+Cy)\,|v_{12}-2v_{22}|}{2U} \tag{24}$$

If we define V^*_{12} as the characteristic field velocity associated with characteristics λ_1 and λ_2, V^*_{12} can be related to γ_{12} in the following manner:

$$\sin\gamma_{12} = V^*_{12}/U \quad \text{for} \quad U \gg V \tag{25}$$

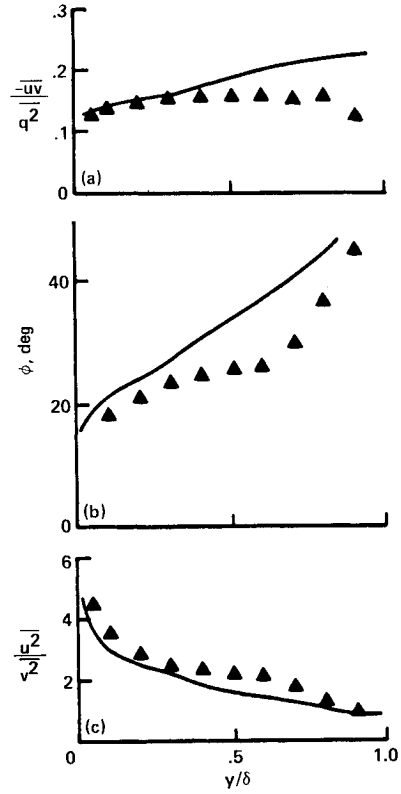

Fig. 5 a) Shear-stress intensity, b) orientation of principal axes of large eddy, and c) anisotropy predicted based on the FVT hypothesis vs y/δ for the flat-plate case: ▲ ▲ Klebanoff.[25]

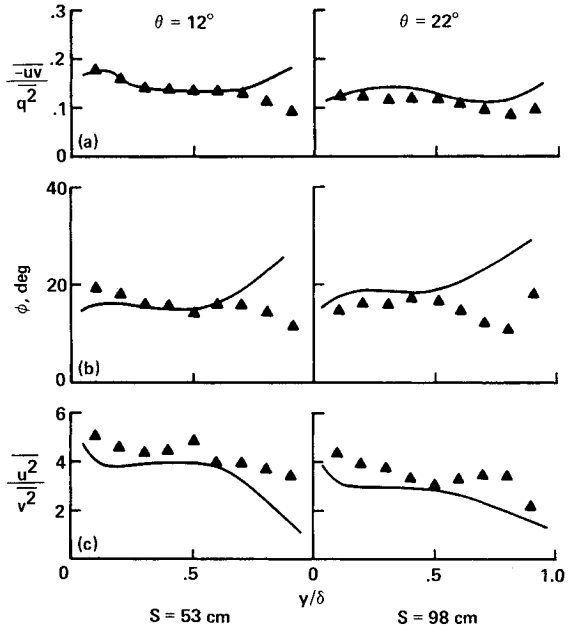

Fig. 6 Turbulence structural quantities vs y/δ for the mild convex case: ▲ ▲ Shivaprasad et al.[27]

Table 2 Values of transport coefficients over the flat recovery wall

Stations, s_f [a] ≅	C_1	C_2	C_3
0.0	2.9	0.74	0.62
1.0δ	2.8	0.90	0.60
10.0δ	2.7	0.92	0.45
∞	2.45	0.95	0.45

[a] s_f is the distance over the flat wall after removal of curvature.

From Eqs. (24) and (25), V_{12}^* is given by the relation

$$V_{12}^* = \tfrac{1}{2}(1+Cy)\,|v_{12} - 2v_{22}| \tag{26}$$

When $v_{12} = 2v_{22}$, the characteristic field velocity becomes zero, as stated earlier.

Considering the three characteristics, λ_1, λ_2, and λ_3 in the x,y plane, one can write in general

$$V_{ij}^* = \tfrac{1}{2}(1+Cy)\,|D_i v_{i2} - D_j v_{j2}| \tag{27}$$
(no Σ for j)

where V_{ij}^* is the characteristic field velocity associated with the λ_i and λ_j characteristics and

$$D_i = 1 \quad \text{for} \quad i = 1 \text{ or } 3$$
$$= 2 \quad \text{for} \quad i = 2 \tag{28}$$

It is of interest to note that the characteristic field velocity for the system of equations employed by Bradshaw et al.[13] becomes

$$V^* = (\tfrac{1}{2}V_c^2 - 2a_1\overline{uv})^{1/2} \tag{29}$$

where V_c and a_1 are the empirical quantities introduced when modeling diffusion of turbulent kinetic energy and turbulent energy itself, respectively. V^* in Eq. (29) then represents the characteristic speed associated with local changes in shear stress.

Removal of Curvature

An interesting test case for the applicability of the LEIM is the so-called relaxing flow case wherein a flow initially subjected to a complex strain such as curvature develops over a flat plate following the curved wall. The central question then pertains to the manner in which turbulence quantities become adjusted to the flat-plate values.

The test case chosen for analysis is due to Gillis et al.,[28] who have reported on measurements in a turbulent boundary layer over a flat plate following a curved wall. The geometrical configuration is shown in Fig. 10. The wall curvature is removed after a 90-deg turn corresponding to a 70-cm flow length (from the start of curved section). The flow, which was initially subjected to a strain by the curved wall, may thus be considered as being in a state of "relaxation" over the flat wall. The nature of changes occurring in the boundary layer following the sudden removal of cur-

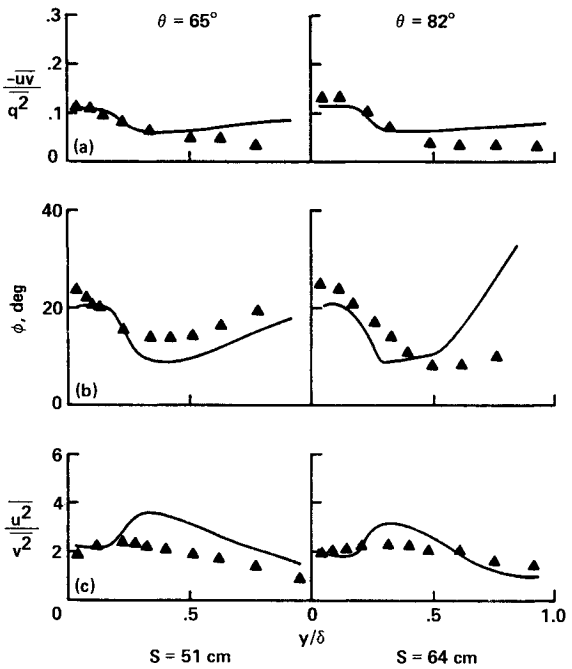

Fig. 7 Turbulence structural quantities vs y/δ for the strong convex case: ▲ ▲ Gillis et al.[28]

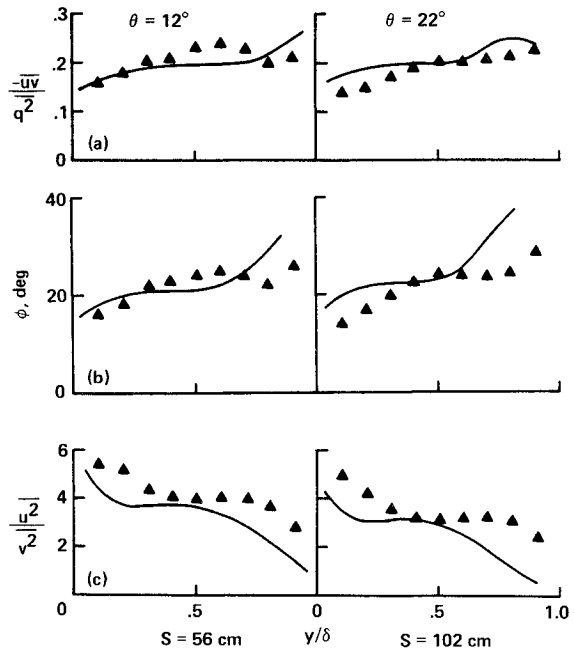

Fig. 8 Turbulence structural quantities vs y/δ for the mild concave case: ▲ ▲ Shivaprasad et al.[27]

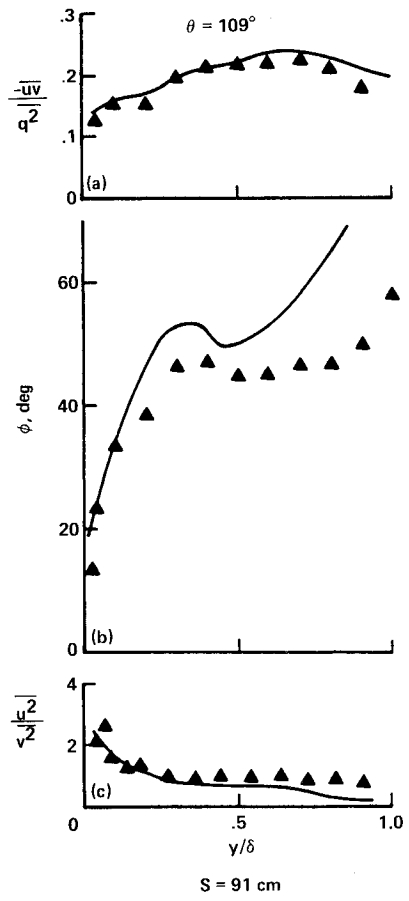

Fig. 9 Turbulence structural quantities for the strong concave case: ▲ ▲ So and Mellor.[29]

vature is obtained utilizing the LEIM based on both the SGD and FVT hypotheses for transport.

In carrying out the predictions over the relaxation region utilizing the SGD hypothesis, we have chosen the values of C_1, C_2, and C_3 which deviate as little as possible from the values for the flat plate case. Such a set of transport coefficients are presented in Table 2. It can be observed therein that in the initial part of the flat plate the values of both C_1 and C_2 need to be different from those for the case of a simple flat plate. The value of C_3 remains unchanged from the value required over the convex wall. As the flow develops downstream over the flat plate the values of C_2 and C_3 become approximately the same as those applicable for the flat-plate case after less than a 10δ distance from the beginning of the flat-wall zone, while the vlaue of C_1 at the end of that distance is still in between the values for the convex wall and the flat plate. Thus, immediately after the curved section, the u component continues to behave similar to that over the convex wall, while the removal of wall curvature seems to affect the v component immediately.

The same flow configuration has also been examined utilizing the FVT hypothesis. The transport velocity scales chosen for the numerical computation are shown in Fig. 11 at three values of y/δ within the outer layer at various stations along the streamwise direction. It can be observed that the values of the transport velocity scales approach those for the flat-plate flow as the flow develops for y/δ values of 0.5 and 0.8. For $y/\delta = 0.2$, however, the values of v_{ij} continue to be different from the values for the flat plate, especially those for the v_{12} component. Thus, the response of the inner part ($y/\delta \cong 0.2$) to the removal of curvature appears to be slower compared to that of the outer part ($y/\delta \cong 0.5$ or 0.8). The three structural quantities, $\overline{uv}/q^2$, ϕ, and $\overline{u^2}/\overline{v^2}$, have been deduced from the data of Gillis et al.[28] and compared with predictions for the outer part of the boundary layer in Fig. 12.

It appears from the foregoing that while the LEIM proves to be a useful framework for explaining some of the features of relaxing boundary layers, no inconsistencies have arisen in the use of either of the two transport hypotheses. Further comparison of the two hypotheses is presented in the following section.

Discussion

1) The LEIM, with eddy-eddy interactions representing turbulent transport modeled on the hypothesis of the existence of finite velocity scales, has been shown to be adequate for predicting the classical structural quantities of turbulence in boundary-layer flows past four variously curved walls. The possibility of using anisotropic velocity scales permits a systematic analysis of the effects of convex and concave curvatures as well as the effects of increasing curvature.

2) Although the velocity scales presented in Figs. 1-3 show appreciable differences for the five flows considered at small values of y/δ, it has been found in predictions of basic turbulence structural quantities that small changes in velocity scales do not cause wide alterations—a result also pointed out in Ref. 13. However, although quantities such as anisotropy and orientation of a large eddy depend strongly on transport, it can be observed that V_{ij}^*, the characteristic field velocity, is a function of various velocity scales and, therefore, different combinations of velocity scales can yield the same characteristic velocity and nearly the same transport field. Accordingly, it is suggested that for most boundary-layer flows, the transport coefficients in ϵ_{ij} or v_{ij} corresponding to the flat-plate case can serve well in a first trial.

3) The characteristic field velocity V_{12}^*, presented in Fig. 13 for three different values of y/δ as a function of wall curvature, increases over a convex surface and decreases over a concave wall. Also, it decreases toward the outer edge of a boundary layer. This has implications for the evolution of

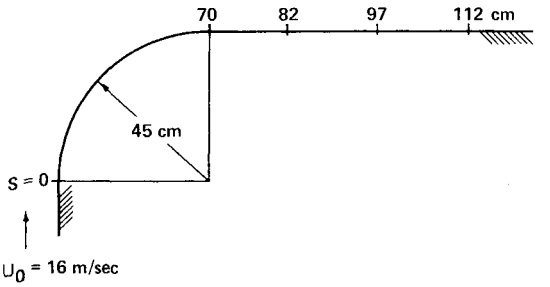

Fig. 10 Geometry of flow over the flat-plate recovery section preceded by the convex wall: Stations along the flow indicate measurement locations.

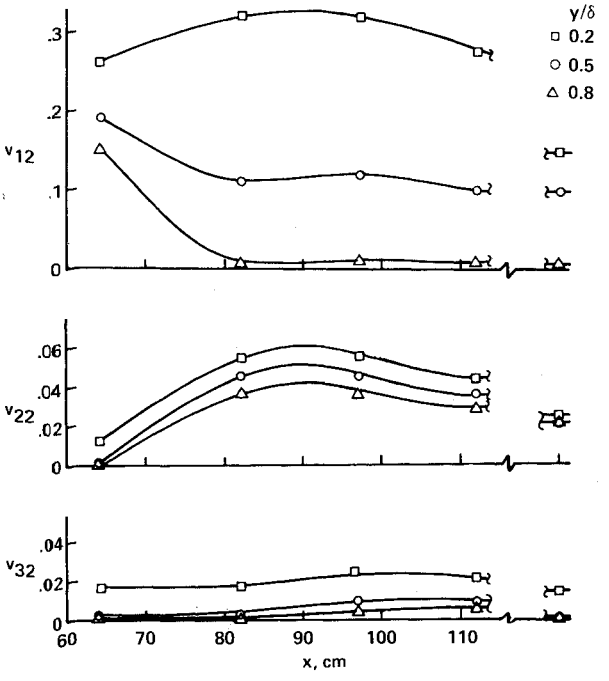

Fig. 11 Changes of transport velocity scales at three values of y/δ along the flow over the flat recovery zone: Points marked denote prediction stations.

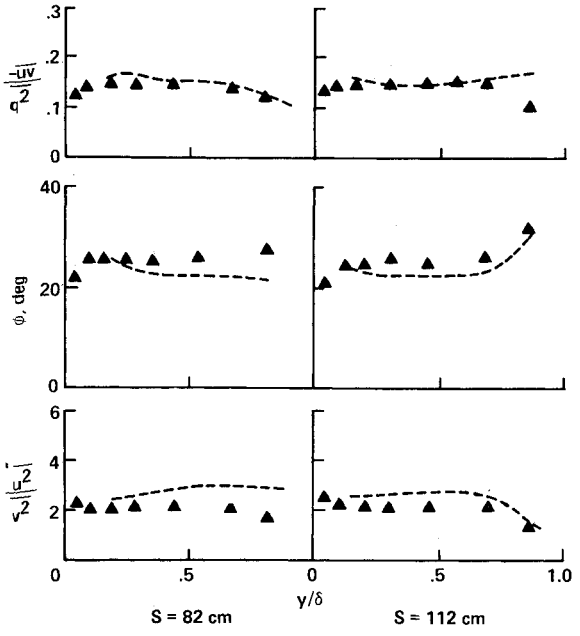

Fig. 12 Three structural quantities predicted based on the FVT hypothesis vs y/δ over the flat recovery zone: ▲ ▲ Gillis et al.[28]

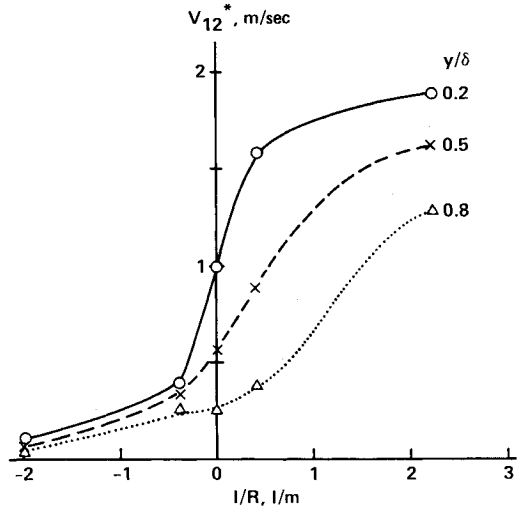

Fig. 13 Characteristic field velocity vs radius of wall curvature at three values of y/δ.

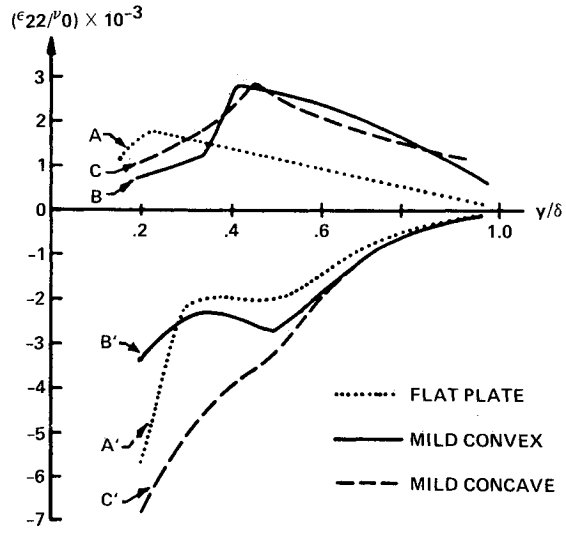

Fig. 14 Comparison of the eddy-viscosity component actually used in the SGD calculation (curves A, B, and C) with that deduced from Eq. (31) (curves A′, B′, and C′).

intermittency, and perhaps also for the setting-in of instability over a concave wall.

4) The LEIM also provides a means of establishing the manner in which turbulence, particularly in anisotropy, becomes relaxed in a boundary layer over a flat plate following development over a curved wall.

5) The gradient diffusion hypothesis represents eddy-eddy interactions as corresponding to diffusion (and dissipation) by the action of eddy viscosity. On the other hand, the current FVT hypothesis introduces the concept of transport as advection with finite velocity scales. Thus, there is a fundamental difference between the two hypotheses.

At the same time, by relating the two scales ϵ_{ij} and v_{ij} in the following manner, namely,

$$\epsilon_{11} = \ell_1^2 \frac{\partial U}{\partial y} = v_{12}(\phi_1^{(1)} + \phi_2^{(1)}) \Big/ \left(\frac{\partial \phi_1^{(1)}}{\partial y} + \frac{\phi_1^{(1)}}{R}\right) \tag{30}$$

$$\epsilon_{22} = \ell_2^2 \frac{\partial U}{\partial y} = v_{22}\phi_2^{(1)} \Big/ \frac{\partial \phi_2^{(1)}}{\partial y} \tag{31}$$

$$\epsilon_{33} = \ell_3^2 \frac{\partial U}{\partial y} = v_{32}(\phi_2^{(1)} + \phi_3^{(1)}) \Big/ \frac{\partial \phi_3^{(1)}}{\partial y} \tag{32}$$

where v_{ij} and $\phi_i^{(1)}$ are functions of wall curvature, it is possible to compare the eddy-viscosity values so deduced for different wall flow cases. As an illustration, ϵ_{22} deduced for the flat-plate, mild convex, and mild concave cases is shown in Fig. 14. Several observations may be made based on that figure. First, ϵ_{22}, when obtained from the first relation of Eq. (31), becomes positive, whereas that deduced from the second relation of Eq. (31) becomes negative in the outer layer. Second, the SGD hypothesis is based on the existence of finite eddy viscosity, but Eq. (31) suggests an infinite value of eddy viscosity corresponding to the peak values of $\phi_i^{(1)}$ distributions with respect to y/δ. This can be seen clearly in Fig. 14. The use of the SGD hypothesis in the outer layer for the eddy-eddy interactions in the form of Eq. (7) contains such paradoxes and, hence, has been considered questionable (Ref. 3, p. 66; Ref. 31, p. 372).

On the other hand, the FVT hypothesis is also subject to several criticisms (for example, Ref. 15, pp. 295-298). In the current application of the FVT hypothesis, no assumptions have been introduced a priori with respect to isotropy; the scales are determined for the outer layer in all three coordinate directions. Furthermore, in the current incompressible flows there has been no need to model pressure-induced effects. However, there are still ambiguities: 1) the gradient of (the first eigenmode of) pressure fluctuation and 2) the velocity scales as functions of y/δ [Eq. (14)]. Such functions for v_{ij} are valid only when there exists some degree of similarity along the flow (Ref. 15, p. 295). Nevertheless, the velocity scales and turbulence quantities based upon those scales do not lead to any basic paradoxes such as those arising in the case of the SGD hypothesis.

6) Finally, it is interesting to observe in this connection that the characteristic field velocity for turbulent transport of the temperature field in a mixing layer[32] can be reduced to

$$V^* = \overline{v^2} \tag{33}$$

where $\overline{v^2}$ is the constant of proportionality introduced in modeling triple correlations; it is also equal to the turbulent normal stress. Now, if one assumes isotropy in transport velocity scales, i.e., $v_{12} = v_{22} = v_{32}$, then the characteristic field velocity in Eq. (26) reduces to

$$V^* = \tfrac{1}{2} v_{22} \tag{34}$$

Thus, the role of the transport velocity scales, v_{ij}, in the transport of eddy-eddy interactions of all sizes, is analogous to that of $\overline{v^2}$ in the transport of temperature fluctuations; the characteristic field velocities of transport are obviously different for the two quantities.

Acknowledgment

The research project reported herein has been carried out under Contract N-78-C-0710 awarded by the Office of Naval Research, under the cognizance of Dr. A. D. Wood. Grateful acknowledgment is made for this support.

References

[1]Launder, B. E. and Spalding, D. B., *Mathematical Models of Turbulence*, Academic Press, New York, 1972.

[2]Cebeci, T. and Smith, A. M. O., *Analysis of Turbulent Boundary Layers*, Academic Press, New York, 1974.

[3]Bradshaw, P., Cebeci, T., and Whitelaw, J. H., *Engineering Calculation Methods for Turbulent Flow*, Academic Press, New York, 1981.

[4]Reynolds, W. C., "Computation of Turbulent Flows," *Annual Review of Fluid Mechanics*, edited by M. Van Dyke et al., Annual Reviews Inc., Palo Alto, CA, Vol. 8, 1976, pp. 183-208.

[5]Cebeci, T., "Wall Curvature and Transition Effects in Turbulent Boundary Layers," *AIAA Journal*, Vol. 9, Sept. 1971, pp. 1868-1870.

[6]Launder, B. E., Priddin, C. H., and Sharma, B. I., "The Calculation of Turbulent Boundary Layers on Spinning and Curved

Surfaces," *Journal of Fluids Engineering*, Vol. 991, 1977, pp. 231-239.

[7]Saffman, P. G., "A Model for Inhomogeneous Turbulent Flows," *Proceedings of the Royal Society, London*, Vol. A317, No. 1530, 1970, pp. 417-433.

[8]Rodi, W., "A New Algebraic Relation for Calculating the Reynolds Stresses," *ZAMM*, Vol. 56, 1976, pp. T219-T221.

[9]Hong, S. K., "Large Eddy Interactions in Curved Wall Boundary Layers—Model and Implications," Ph.D. Thesis, Purdue University, West Lafayette, IN, Aug. 1983.

[10]Hong, S. K. and Murthy, S. N. B., "Structure of Turbulence in Curved Wall Boundary Layers," AIAA Paper 83-0457, Jan. 1983.

[11]Hong, S. K. and Murthy, S. N. B., "Pressure-Strain Correlations in Curved Wall Boundary Layers," AIAA Paper 84-1671, June 1984.

[12]Sreenivasan, K. R., Tavoularis, S., and Corrsin, S., "A Test of Gradient Transport and Its Generalizations," *Turbulent Shear Flows 3*, edited by L. J. S. Bradbury et al., Springer-Verlag, New York, 1982, pp. 96-112.

[13]Bradshaw, P., Ferriss, D. H., and Atwell, N. P., "Calculation of Boundary-Layer Development Using the Turbulent Energy Equation," *Journal of Fluid Mechanics*, Vol. 28, March 1967, pp. 593-616.

[14]Townsend, A. A., *The Structure of Turbulent Shear Flow*, 1st Ed., Cambridge Univ. Press, London, 1956.

[15]Townsend, A. A., *The Structure of Turbulent Shear Flow*, 2nd Ed., Cambridge Univ. Press, London, 1976.

[16]Corrsin, S., "Limitations of Gradient Transport Models in Random Walks and in Turbulence," *Advances in Geophysics*, edited by H. E. Landsburg et al., Academic Press, New York, pp. 25-60.

[17]Lumley, J. L., "The Structure of Inhomogeneous Flows," *Atmospheric Turbulence and Radio Wave Propagation*, edited by A. M. Yaglom and V. I. Tartarsky, Publishing House NAUKA, Moscow, 1967, pp. 166-176.

[18]Payne, F. R. and Lumley, J. L., "Large Eddy Structure of the Turbulent Wake Behind a Circular Cylinder," *The Physics of Fluids*, Vol. 10, 1967, pp. S194-S196.

[19]Lemmerman, L. A. and Payne, F. R., "Extraction of the Large Eddy Structure of a Turbulent Boundary Layer," AIAA Paper 77-717, 1977.

[20]Townsend, A. A., "Entrainment and the Structure of Turbulent Flow," *Journal of Fluid Mechanics*, Vol. 41, April 1970, pp. 13-46.

[21]Mathieu, J. and Jaendel, D., "Pathological Cases in Turbulent Field and Spectral Approach," *von Kármán Institute for Fluid Dynamics Lecture Series*, 1979-2, 1979.

[22]Hong, S. K., "Large Eddy Interactions in Turbulent Channel Flow," NASA-TM-86757, Sept. 1985.

[23]Boussinesq, J., "Essai sur la Theorie des Eaux Courantes," *Mem. Pres. par Div. Savants a l'Acad Sci.*, Paris, Vol. 23, No. 1, 1877, pp. 1-680.

[24]Loitsyanskii, L. G., "Memory Effects in Turbulent Motions," *Fluid Dynamics*, Vol. 17, No. 2, 1982, pp. 167-179.

[25]Klebanoff, P. S., "Characteristics of Turbulence in a Boundary Layer with Zero Pressure Gradient," NACA TN-3178, 1954.

[26]Ramaprian, B. R. and Shivaprasad, B. G., "Mean Flow Measurements in Turbulent Boundary Layers Along Mildly Curved Surfaces," *AIAA Journal*, Vol. 15, Feb. 1977, pp. 189-196.

[27]Shivaprasad, B. G. and Ramaprian, B. R., "Turbulence Measurements in Boundary Layers Along Mildly Curved Surfaces," *Journal of Fluids Engineering*, Vol. 100, March 1978, pp. 37-46.

[28]Gillis, J. C., Johnston, J. P., Moffat, R. J., and Kays, W. M., "Experimental Data and Model for the Turbulent Boundary Layer on a Convex, Curved Surface," NASA CR-3391, 1981.

[29]So, R. M. C. and Mellor, G. L., "An Experimental Investigation of Turbulent Boundary Layers Along Curved Surfaces," NASA CR-1940, 1972.

[30]Greenspan, D., *Discrete Numerical Methods in Physics and Engineering*, Academic Press, New York, 1974, pp. 250-254.

[31]Hinze, J. D., *Turbulence*, 2nd Ed., McGraw-Hill Book Co., New York, 1975.

[32]Kurbatskii, A. F. and Yanenko, N. N., "On the Modeling of Effects of Negative Production of Temperature-Fluctuation Intensity in the Turbulent Mixing Layer," *Journal of Fluid Mechanics*, Vol. 130, Sept. 1983, pp. 453-462.